View metadata, citation and similar papers at core.ac.uk

brought to you by CORE

provided by INRIA a CCSD electronic archive server

Image-based motion detection in 4D images and application to respiratory motion suppression

Marine Breuilly, Grégoire Malandain, Nicholas Ayache, Julien Guglielmi, Thierry Pourcher, Philippe Franken, Jacques Darcourt

To cite this version:

Marine Breuilly, Grégoire Malandain, Nicholas Ayache, Julien Guglielmi, Thierry Pourcher, et al.. Image-based motion detection in 4D images and application to respiratory motion suppression. ISBI - International Symposium on Biomedical Imaging, Apr 2013, San Francisco, United States. pp.792-795, 10.1109/ISBI.2013.6556597 . hal-00799368

HAL Id: hal-00799368

https://hal.inria.fr/hal-00799368

Submitted on 12 Mar 2013

HAL is a multi-disciplinary open access archive for the deposit and dissemination of scientific research documents, whether they are published or not. The documents may come from teaching and research institutions in France or abroad, or from public or private research centers.

L'archive ouverte pluridisciplinaire **HAL**, est destinée au dépôt et à la diffusion de documents scientifiques de niveau recherche, publiés ou non, émanant des établissements d'enseignement et de recherche français ou étrangers, des laboratoires publics ou privés.

IMAGE-BASED MOTION DETECTION IN 4D IMAGES AND APPLICATION TO RESPIRATORY MOTION SUPPRESSION

M Breuilly[⋆†]*, G Malandain*[⋆]*, N Ayache*[⋆]*, J Guglielmi*[†]*, T Pourcher*[†]*, PR Franken*[†]*, J Darcourt*[†]

[⋆] Inria Sophia Antipolis - Méditerranée, Sophia Antipolis, France
[†]Laboratoire TIRO, Commissariat à l'Énergie Atomique et aux Énergies Alternatives (CEA) / Université de Nice Sophia-Antipolis / Centre Antoine Lacassagne, Nice, France

ABSTRACT

Respiratory motion may blur the tomographic reconstruction of PET or SPECT images, which subsequently impairs quantitative measurements, e.g. in the upper abdomen area. Respiratory phase-based gated reconstruction addresses this problem for CT images, but deteriorates the signal-to-noise ratio and other intensity-based quality measures for ET images.

This article describes an image-based motion detection method for dynamic images, which works for both 4D-CT and 4D-SPECT images. This method allowed us to identify the motionless phases from the image-based motion signal. Interestingly, we found that the peak of motion according to the pressure signal, recorded during the acquisition and considered as a reference, is temporally shifted compared to the motion-phases identified by the proposed method. Moreover, these observations permit to reconstruct a breath hold like 3D SPECT image improving the quality of the 3D reconstruction compared to both 4D reconstruction and standard 3D reconstruction.

Index Terms— small animal imaging, single photon emission computed tomography, respiratory motion detection

1. INTRODUCTION

Emission tomography (ET) is an efficient imaging tool for physiological and functional processes. It provides *in vivo* information and allows longitudinal studies. For such studies, qualitative analysis may not be sufficient to reveal subtle differences between groups (for instance, in oncological studies where different therapy strategies have to be assessed), and quantitative analysis is thus necessary. ET quantification may be impaired by physical (e.g. attenuation, etc) or physiological (e.g. motion) causes. Methods exist to take care of the former both for Positron Emission Tomography (PET) or Single-Photon Emission Computed Tomography (SPECT) [1]. Motion compensation, however, is still an active research topic.

In ET imaging, motion artefacts can be handled by gating protocols. An additional signal, which is considered representative of the motion of interest, is recorded and synchronised with the data acquisition. Reconstruction is then based on a selection of the acquired data. Such signals can be acquired by an external device and include electrocardiogram [2], Real-time Position Management [3] or Multidimensional Respiratory Gating [4], and pressure sensor (chest belt) [5, 6].

Phase-based gating divides the period into several phases of equal duration, with the assumption that the motion can be neglected within each phase. This method is used for both cardiac [7] and respiratory [8] motions and allows the reconstruction of dynamic or 4D (3D+t) images. However, using only a fraction of the acquired data deteriorates the signal-to-noise ratio (SNR) of each 3D image, especially in ET. Therefore, Dawood et al. propose to co-register each 3D image and then to sum them up [9]. This method permits to obtain a 3D image with minimum motion and improved SNR, but assumes that image co-registration can be achieved with minimal error. Another gating approach, amplitude-based gating, assumes that the signal amplitude is representative of the motion of interest. A range of amplitude values is selected, and the associated acquired data are used for reconstruction. For instance, images at end of exhalation or inhalation can be reconstructed by selecting either the lowest or the highest amplitude values of a respiratory representative signal. In human imaging, such a method has been used for respiratory motion in PET [5, 4, 6]. In the case when a motion model is available, some authors proposed to incorporate the model into the tomographic reconstruction procedure in order to take into account all the acquired data to reconstruct a 3D still image. In human imaging, cardiac [10] and respiratory [11, 12] motion models have been developed. In addition to the difficulty in defining an accurate motion model, such methods also imply a huge computational cost.

The motivation of our work is the oncological studies in a molecular pre-clinical imaging context, for tumours in the upper abdominal area. Therefore, motion artefacts have to be reduced before conducting any quantitative studies. While motion compensation has been widely studied in human imaging, the literature is less abundant for pre-clinical imaging and mostly concerns μ-CT [13, 14]. The proposed method will take advantage of the particular respiratory pattern of the anaesthetized mice (still periods separated by gasping breaths

[15]). Detecting the gasping breaths allows in turn to select the still periods and to use the associated data to reconstruct a motion-free 3D image. However, it appeared that the acquired respiratory representative signal (here a pressure signal) is not representative of the respiratory motion. Therefore it motivates an ad-hoc image based motion detection.

2. IMAGING PROTOCOL

We acquired experimental animal images (both SPECT and CT) using a dedicated small animal SPECT/CT scanner (eXplore speCZT CT 120, GE Healthcare Bioscience, London ON, CA). SPECT and CT camera are located on two different gantry. Thus the system does not allow synchronous SPECT and CT images acquisition and SPECT and CT images have to be registered with a known global rigid transformation (translation). The output of the SPECT camera is a list-mode of all events detected on the detectors: every millisecond, the time, the gating index, and the properties of all detected photons are recorded.

A monitoring system (BioVet, m2m Imaging Corporation, Newark, USA) was used with a pneumatic pressure sensor placed under the animal abdomen. The pressure signal was recorded (1 ms-sampled rate) and used to monitor the animal anaesthesia. Body temperature was maintained at 37°Celsius and anaesthetized gas rate was regularly controlled to keep the respiratory rate between 60 and 100 breaths per minute. Once a stabilized respiratory rate was reached, the image acquisition started.

At the beginning of each acquisition, an amplitude threshold was arbitrarily fixed in order to detect the rising edge of the pressure signal variation. Each time the signal passes this threshold, a trigger is sent to the camera. In the SPECT mode, this trigger is recorded in the list-mode to be used for latter gated reconstruction. We assume that this trigger corresponds to the same time in the cycle for each respiratory cycle. A respiratory cycle is then defined by the interval between two consecutive triggers in the SPECT list-mode. In the gated CT mode, every trigger initiated the acquisition of a projection.

3. MOTION DETECTION

The principle of the proposed method is to detect, from a first 4D reconstruction, the phases exhibiting some motion, and then to discard the data associated with those phases in the final reconstruction. For CT images, the 4D sequence reconstructed by the constructor software is sufficient to detect these phases. However, some extra work has to be conducted for the reconstruction of 4D SPECT images.

3.1. 4D SPECT image reconstruction

From the recorded triggers in the SPECT list-mode data, we compute the mean $\overline{C}$ and the standard deviation σ of the respiratory cycle length. The data associated with cycles outside $\pm 3\sigma$ are discarded because we suspect that they are associated with some respiratory artefacts. This concerns around 3% of the data.

Then, since the respiratory cycles exhibit some length variation, we build cycles of uniform length $\overline{C}_s$ by redistributing the data of each cycle into a cycle of length $\overline{C}_s$. $\overline{C}_s$ is chosen as the closest value to $\overline{C}$, that is a multiple of the number N of phases being reconstructed. This way we ensure that each respiratory cycle will be correctly binned in the right number of phases. The i^{th} cycle is defined by the interval $[t_i, t_{i+1}[$ where t_i is the time of the i^{th} trigger. The events in the list mode data associated to time t in this interval will now be associated to time t' defined by

$$t' = (i-1)\overline{C}_s + (t - t_i)\frac{\overline{C}_s}{t_{i+1} - t_i} \quad (1)$$

Then it is straightforward to reconstruct a 4D image of N phases from this new list-mode. However, the number of detected events differs from one reconstructed phase to the other. Thus, we normalized all the reconstructed phases with respect to one reference phase by multiplying the voxel intensities by the number of events used in the reference phase divided by the number of events used in the considered image.

3.2. 4D image analysis

The principle of the method is that the voxels reconstructed at the position $\mathbf{x}$ will exhibit some intensity variation if they are located in an area containing a moving edge. Given a 4D image made of N 3D phase images I_n, $n \in [1, N]$, we compute an amplitude image A such that :

$$\forall \mathbf{x} : A(\mathbf{x}) = \max\{I_n(\mathbf{x})\}_{n\in[1,N]} - \min\{I_n(\mathbf{x})\}_{n\in[1,N]} \quad (2)$$

This amplitude image will have high intensity values at the location of the moving edges. This image is then thresholded to keep only the regions of potential motion, generating a mask M. A threshold at 15% (resp. 30%) of the maximum amplitude was arbitrarily chosen for SPECT (resp. CT) images.

According to the pressure signal, we observed that around 2/3 of the respiratory cycles do not exhibit significant motion. Since N phases are reconstructed, with $N = 15$, this corresponds to around 10 phases without motion; the 5 other phases are the cause of the intensity variations due to motion. Therefore, for each voxel $\mathbf{x} \in M$, we compute the amplitude after discarding every possible sequence of 5 consecutive phases. We define S_m as a sequence of 5 consecutive phases:

$$S_m = \{k \in [1, N] | \exists j \in [0, 4] : k - m \equiv j[N]\} \quad (3)$$

The discarded sequence yielding the smallest amplitude is associated to a possible motion under the considered voxel. This sequence is defined by its first phase $\hat{m}(\mathbf{x})$ computed by:

$$\hat{m}(\mathbf{x}) = \arg \min_{m\in[1,N]} (\max\{I_n(\mathbf{x})\}_{[1,N]\setminus S_m} - \min\{I_n(\mathbf{x})\}_{[1,N]\setminus S_m}) \quad (4)$$

We cumulated the obtained sequences $S_{\hat{m}(\mathbf{x})}$ into a histogram:

$$\forall n \in [1, N],\ h(n) = card\{\mathbf{x} \in M / n \in S_{\hat{m}(\mathbf{x})}\} \quad (5)$$

The resulting histogram h is automatically thresholded [16], yielding two groups of phases. The smallest group (typ. 5 to 6 phases) is associated with motion state and the largest group (typ. 10 or 9 phases) is associated with the motionless state. In the latter group, $\hat{p}$ denotes the first phase and L denotes the number of phases of the largest group.

4. RESULTS

4.1. Detected motion

Interestingly, the observed motion in gated 4D images appeared to be temporally shifted with respect to the pressure signal. This observation motivated the proposed ad-hoc image-based motion detection method. To exemplify this, we have compared the proposed motion detection method, applied to both SPECT and CT 4D images, to the lung volume (extracted from CT) and to the pressure signal.

For this experiment[1], one healthy C57BL6 female mouse (weighing 26 g) was injected intra-peritoneally 100 MBq in 400 μL of ^{99m}Tc-pertechnetate. SPECT and 4D-CT images have been acquired one after the other. Both of the modalities acquisitions was synchronised to the pressure signal.

Motion was detected from 4D SPECT image using the proposed method. We observed that the peak of the detected motion (i.e. the phase that belongs to a majority of discarded sequences $S_{\hat{m}}$) is temporally shifted with respect to the pressure signal peak. As a consequence, the phases resulting from a threshold of the histogram $h(n)$ differed from the ones that would have resulted from a threshold of the pressure signal. Changing the length of the discarded sequences (data non presented here) did not change the location of the peak. The same motion detection method has been applied to the 4D CT images, and the peak of the motion also appeared at the same phase. Last, we have computed the lung volume along the phases with an ad-hoc and simple method (Gaussian smoothing, threshold between -650 HU and -250 HU, and morphological closing). Again the peak of volume variation appeared at the same phase. Figure 1 presents the result of all image-based motion detection and illustrates the temporal shift between the normalized average pressure signal (continuous black curve) and a set of different image-based results: normalised histogram $h_{4D-SPECT}(n)$ computed on the 4D-SPECT image (blue staircase), normalised histogram $h_{4D-CT}(n)$ of motion phase computed on the 4D-CT image (red curve with cross-shaped markers), and lung volume (mL) measured on the 4D-CT image (black dotted curve with circle-shaped markers).

[1] Animal housing and procedures were conducted according to the guidelines of the French Agriculture Ministry and were approved by the local ethics committee.

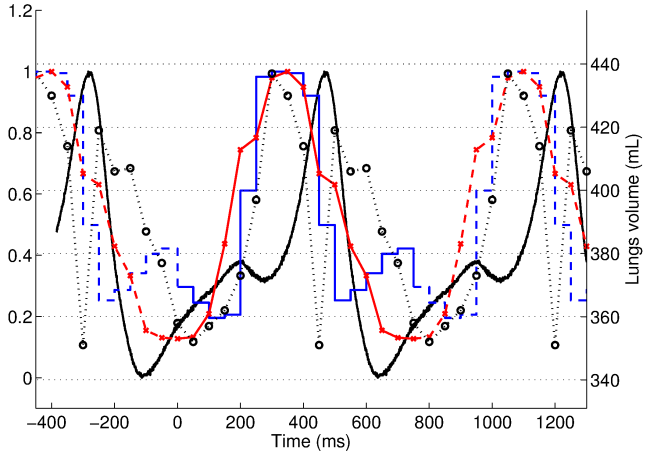

Fig. 1. Image-based motion signal from 4D-SPECT and 4D-CT image compared to the pressure signal and lung volume variation.

The value of the temporal shift between the motion observed in images and the pressure variation did not seem to be predictable between animals or acquisitions. We suspect that are many contributing causes, including the placement of the pressure sensor.

4.2. Reconstruction of breath-hold like SPECT images

One NOD-SCID female mouse[1] (weighing 17.7 g) was injected intra-peritoneally 1.5 million cells of rat colonic adenocarcinoma expressing the Natrium Iodide Symporter (PROb-mNIS) in 50μL of Phosphate Buffered Saline. After 3 weeks of growth, this mouse was injected intra-peritoneally 180 MBq in 400 μL of ^{99m}Tc-pertechnetate and was scanned with both SPECT and 3D-CT. On the SPECT, PROb-mNIS peritoneal nodules of NIS-transfected cells were visible, some of them located just under the diaphragm.

We applied the proposed method on the reconstructed 4D-SPECT image. Extracting the motionless phases allowed the reconstruction of a breath-hold like 3D image (BH3D). For this image, only the data belonging to motionless phases are used. That is, for each cycle, all data from the phase $\hat{p}$ and for a time interval of length $L \times \overline{C}_s/N$, this corresponds roughly to 2/3 of the original data. Figure 2 assesses the quality of the first results. First, BH3D image is less noisy than the 4D images at the end of exhalation or at the end of inhalation. Second, the zoomed-in view of the lesion is less blurred in BH3D than in the standard 3D image.

5. CONCLUSION

In this paper, we presented an image-based motion detection method for dynamic images. We extracted a discrete motion signal from the analysis of high intensity variation regions

in dynamic images and compared it to the original pressure signal. This method has been tested on two imaging modalities, CT and SPECT. For both, we obtained similar image-based motion signals. Moreover, a temporal shift between the peak of motion in the pressure signal and the peaks in the two image-based signals has been demonstrated, that justified posteriorly such an image-based motion detection approach.

This temporal shift has been confirmed by lung volume variation in the 4D-CT. Although the proposed method is quite simple, it achieved good results. Moreover, it allowed the reconstruction of breath-hold like 3D SPECT image.

For future work, the proposed method will be used on more SPECT images in order to reconstruct motionless 3D images. This will allow us to evaluate our method both qualitatively and quantitatively compared to other SPECT reconstruction schemes.

6. REFERENCES

[1] P Ritt, H Vija, J Hornegger, and T Kuwert, "Absolute quantification in SPECT.," *Eur J Nucl Med Mol Imaging*, 2011.

[2] L Livieratos, K Rajappan, L Stegger, K Schäfers, DL Bailey, and PG Camici, "Respiratory gating of cardiac PET data in list-mode acquisition.," *Eur J Nucl Med Mol Imaging*, 2006.

[3] N Grotus, AJ Reader, S Stute, JC Rosenwald, P Giraud, and I Buvat, "Fully 4D list-mode reconstruction applied to respiratory-gated PET scans.," *Phys Med Biol*, 2009.

[4] SA Nehmeh et al., "A novel respiratory tracking system for smart-gated PET acquisition.," *Med Phys*, 2011.

[5] G Chang, T Chang, T Pan, JW Clark, and OR Mawlawi, "Implementation of an automated respiratory amplitude gating technique for PET/CT: clinical evaluation.," *J Nucl Med*, 2010.

[6] W van Elmpt et al., "Optimal gating compared to 3D and 4D PET reconstruction for characterization of lung tumours.," *Eur J Nucl Med Mol Imaging*, 2011.

[7] F Büther et al., "Detection of respiratory tumour motion using intrinsic list mode-driven gating in positron emission tomography.," *Eur J Nucl Med Mol Imaging*, 2010.

[8] RA Bundschuh, A Martinez-Moller, M Essler, SG Nekolla, SI Ziegler, and M Schwaiger, "Local motion correction for lung tumours in pet/ct–first results.," *Eur J Nucl Med Mol Imaging*, 2008.

[9] M Dawood, N Lang, X Jiang, and KP Schäfers, "Lung Motion Correction on Respiratory Gated 3-D PET/CT Images," *IEEE Trans Med Imaging*, 2006.

[10] C Blondel, R Vaillant, G Malandain, and N Ayache, "3-d tomographic reconstruction of coronary arteries using a precomputed 4-d motion field.," *Phys Med Biol*, 2004.

[11] F Lamare et al., "List-mode-based reconstruction for respiratory motion correction in PET using non-rigid body transformations.," *Phys Med Biol*, 2007.

[12] M Reyes, G Malandain, PM Koulibaly, MA Gonzalez-Ballester, and J Darcourt, "Model-based respiratory motion compensation for emission tomography image reconstruction.," *Phys Med Biol*, 2007.

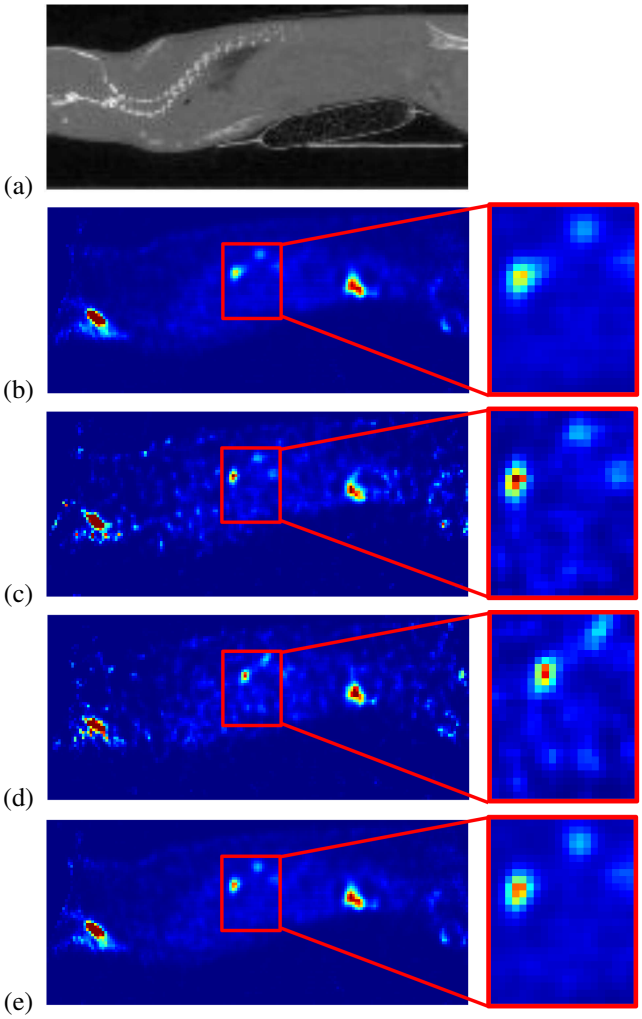

Fig. 2. Sagittal views from sub-diaphragmatic peritoneal lesions comparing standard 3D, G4D, and BH3D SPECT reconstruction methods. Left column: anatomical reference CT image (a), standard 3D reconstruction (b), end-of-exhalation phase from 4D reconstruction (c), end-of-inhalation phase from 4D reconstruction (d), BH3D reconstruction (e); Right column: zoomed-in on a region with lesions of interest of the SPECT images. The same SUV scale has been used for all SPECT images.

[13] X Guo, SM Johnston, Y Qi, GA Johnson, and CT Badea, "4D micro-CT using fast prospective gating.," *Phys Med Biol*, 2011.

[14] L Martiniova, D Schimel, EW Lai, A Limpuangthip, R Kvetnansky, and K Pacak, "In vivo micro-ct imaging of liver lesions in small animal models.," *Methods*, 2010.

[15] D Cavanaugh, E Johnson, RE Price, J Kurie, EL Travis, and DD Cody, "In vivo respiratory-gated micro-ct imaging in small-animal oncology models.," *Mol Imaging*, 2004.

[16] N Otsu, "A threshold selection method from gray-level histograms," *IEEE Trans Syst Man Cyb*, 1975.